Electronic Supplementary Material (ESI) for ChemComm.
This journal is © The Royal Society of Chemistry 2014

Synthesis and Characterization of a Mercury-Containing Trimetalloboride

Supplementary Information

Rüdiger Bertermann, Holger Braunschweig*, William C. Ewing, Thomas Kramer, Ashwini K. Phukan, Alfredo Vargas, and Christine Werner

Institut für Anorganische Chemie, Julius-Maximilians Universität Würzburg, Am Hubland, D-97074 Würzburg, Germany.

To whom correspondence should be addressed:

E-mail: h.braunschweig@uni-wuerzburg.de

Tel: +49-(0)931/31–85260. Fax: +49-(0)93 /31–84623.

Experimental section

All manipulations were performed either under an atmosphere of dry argon or in vacuo using standard Schlenk line or glovebox techniques. NMR spectra in solution were acquired on Bruker Avance I 500 (^{1}H: 500.1 MHz, ^{11}B: 160.5 MHz, ^{13}C: 125.8 MHz, ^{199}Hg: 89.6 MHz) and Bruker Avance III HD 300 (^{1}H: 300.2 MHz, ^{11}B: 96.3 MHz, ^{199}Hg: 53.8 MHz) FT-NMR spectrometers. ^{1}H NMR and ^{13}C{^{1}H} NMR spectra were referenced to external TMS via residual protons of the solvent (^{1}H) or the solvent itself (^{13}C). ^{11}B{^{1}H} NMR spectra were referenced to external $BF_3{\cdot}OEt_2$, while ^{199}Hg{^{1}H} and ^{199}Hg{^{1}H, ^{11}B} NMR spectra were referenced to external $HgMe_2$. The ^{199}Hg NMR spectra at 53.8 MHz were recorded at 298 K with 52,000 scans, an acquisition time of 0.2 s, and a sufficient recycle delay (2 s) using a 5 mm triple resonance observe Probe (TBO BB-^{1}H-^{11}B) with proper frequency filters. The observed spin-system in the ^{199}Hg{^{1}H} NMR spectrum (89.6 MHz) of compound **3** was fitted using WINDAISY 4.05 from Bruker-Franzen Analytik GmbH. IR spectra were acquired on a JASCO FT/IR-6200 type A spectrometer. Elemental analysis was performed on a Leco CHNS-932 Elemental Analyzer.

Materials: Dimetalloborylene **1** $Li^+[(Cp_2(CO)_4Mn_2)B]^-$ was prepared as previously described.[1] Phenylmercuric chloride (Aldrich) was used as received. All solvents were purified by distillation from appropriate drying agents and stored under argon over molecular sieves. Deuterated solvents were dried under an argon atmosphere over molecular sieves and degassed by three freeze-pump-thaw cycles.

Synthesis of $(Cp_2(CO)_4Mn_2)B\text{-}Hg(C_6H_5)$ (3): Phenylmercuric chloride (6.8 mg, 0.022 mmol) was added to a solution of **1** (14 mg, 0.022 mmol) in toluene (1 mL) and stirred for 0.5 h at room temperature. The reaction mixture was observed to change from colorless to bright red, concomitant with the formation of a colorless precipitate and the emergence of a low-field shift at 208 ppm in the ^{11}B NMR spectrum. The solution was filtered, concentrated, and stored at -35 °C. After 12 h, yellow crystals of **3** suitable for X-ray analysis were obtained.[2]
For **3**: 6.0 mg (0.0094 mmol, 43%). NMR: ^{1}H (C_6D_6, 500.1 MHz): $\delta = 7.77$ ($^{3}J_{H-Hg} = 143$ Hz, d, 2H, $o\text{-}H_{Ph}$), 7.42 ($^{4}J_{H-Hg} = 38$ Hz, t, 2H, $m\text{-}H_{Ph}$), 7.19 (t, 1H, $p\text{-}H_{Ph}$), 4.17 (s, 10H, *Cp*). ^{11}B{^{1}H} (C_6D_6, 160.5 MHz): $\delta = 208$. ^{13}C{^{1}H} (C_6D_6, 125.8 MHz): $\delta = 226.0$ (*CO*), 177.2 (s, $ipso\text{-}C_{Ph}$), 136.9 (s, $o\text{-}C_{Ph}$), 129.8 (s, $m\text{-}C_{Ph}$), 128.7 (s, $p\text{-}C_{Ph}$), 82.6 (s, *Cp*). ^{199}Hg{^{1}H} (C_6D_6, 89.6 MHz): $\delta = 83.9$ (br). ^{199}Hg{^{1}H,^{11}B} (C_6D_6, 53.8 MHz): $\delta = 83.9$ (s). FT-IR

(hexane): 1975 (br), 1934 (br), 1882 (br) cm^{-1}. Elemental analysis: calc'd (%) C: 37.50, H: 2.36; found (%) C: 36.80 H: 2.26.

Crystallographic methods for 3. The crystal data for CCDC 975393 were collected on a Bruker X8-APEX II diffractometer with a CCD area detector and multi-layer mirror monochromated Mo$_{K\alpha}$ radiation. The structure was solved using direct methods, refined with the Shelx software package[3] and expanded using Fourier techniques. All non-hydrogen atoms were refined anisotropically. Hydrogen atoms were included in structure factors calculations. All hydrogen atoms were assigned to idealized geometric positions. The 10 of 158 reported least-squares restraints as shown by _refine_ls_number_restraints key are attributed to DELU keyword in ShelXL input ('rigid bond' restraint for all bonds in the connectivity list; standard values of 0.005 for both parameters s1 and s2 were used). The displacement parameters of atoms C16 > C20 and C61 > C65 were restrained to the same value with similarity restraint SIMU.

Crystal data for **3** (CCDC 975393): $C_{20}H_{15}BHgMn_2O_4$, M_r = 640.60, yellow block, 0.21×0.13×0.06 mm^3, Triclinic space group *P*-1, a = 11.7014(9) Å, b = 11.8444(10) Å, c = 14.6285(12) Å, α = 87.903(3)°, β = 80.315(3)°, γ = 74.374(2)°, V = 1924.6(3) Å^3, Z = 4, ρ_{calcd} = 2.211 g·cm^{-3}, μ = 9.273 mm^{-1}, $F(000)$ = 1208, T = 100(2) K, R_1 = 0.0237, wR^2 = 0.0410, 7603 independent reflections [$2\theta \leq 52.04°$] and 551 parameters.

Crystallographic data have been deposited with the Cambridge Crystallographic Data Center as supplementary publication no. CCDC 975393. These data can be obtained free of charge from The Cambridge Crystallographic Data Centre *via* www.ccdc.cam.ac.uk/data_request/cif

Computational Details: Simulated FT-IR data (Fig. S1) was obtained at the B3LYP/6-311G(d) level of theory, with the LANL2DZ pseudopotential applied for Mn an Hg atoms, via frequency calculation with the Gaussian09 program.[4] The geometry was a confirmed minimum, with no imaginary frequencies. The coordinates are given in Table S1. Details for the ETS-NOCV calculations used in this work have been described in the main text (ref. 11). Coordinates used in the ETS-NOCV analysis are given in Tables S2 and S3.

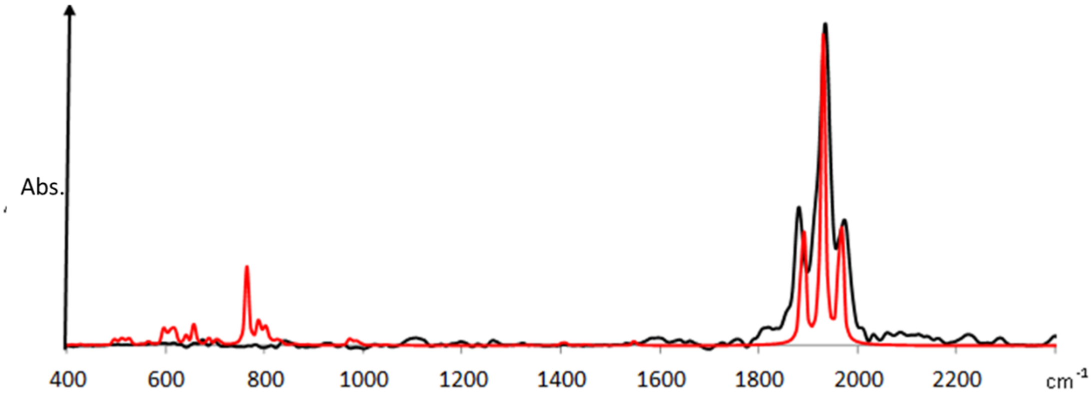

Supplementary Figure S1. Comparison of the measured (—) and calculated (—) IR spectrum of **3** (B3LYP/6-311G(d),LANL2DZ). Absorbance intensities have been scaled, and a fit-factor of 0.96 has been applied to the x-axis of the calculated data.

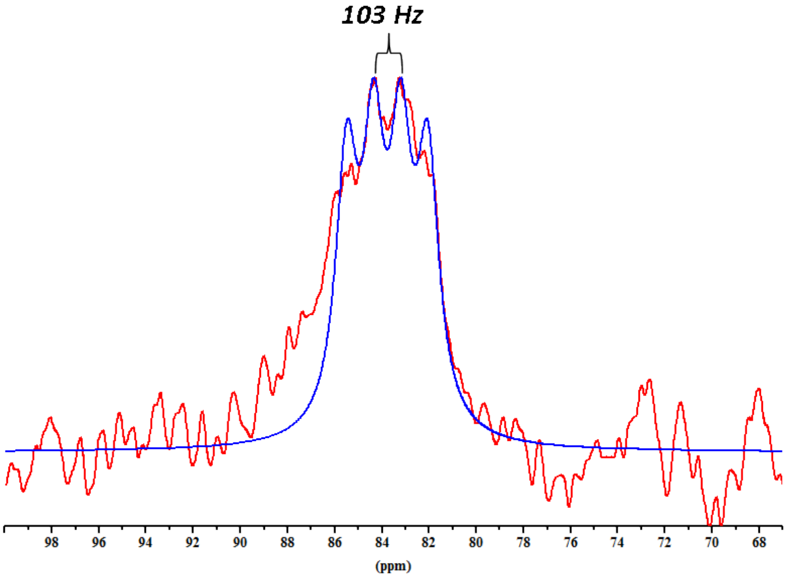

Supplementary Figure S2. The simulated ^{199}Hg{^{1}H} NMR spectrum of **3** with *J*(^{199}Hg,^{11}B) = 103 Hz, fit to data collected at 500 MHz.

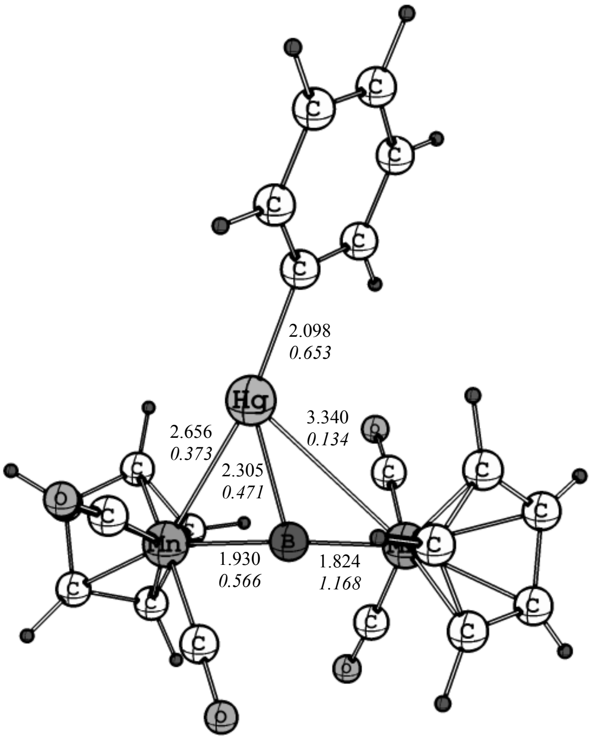

Supplementary Figure S3. Geometry of **3** optimized at the OLYP/TZP,QZ4P level of density functional theory using the ADF program with relevant bond lengths. Values in italics represent the computed Mayer's bond order.

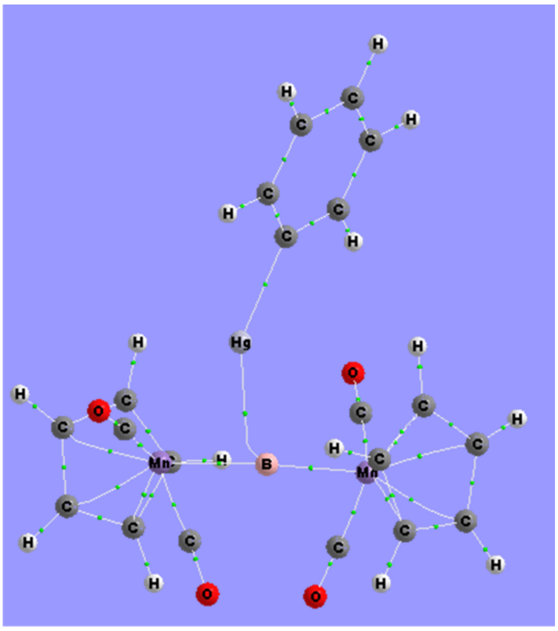

Supplementary Figure S4. QTAIM molecular graph of **3**. Green dots represent bond critical point (BCP). The calculation was performed with the B3LYP DFT functional, using the 6-311+G* basis set for all H, B, C, O, and Mn atoms and SDD for Hg.

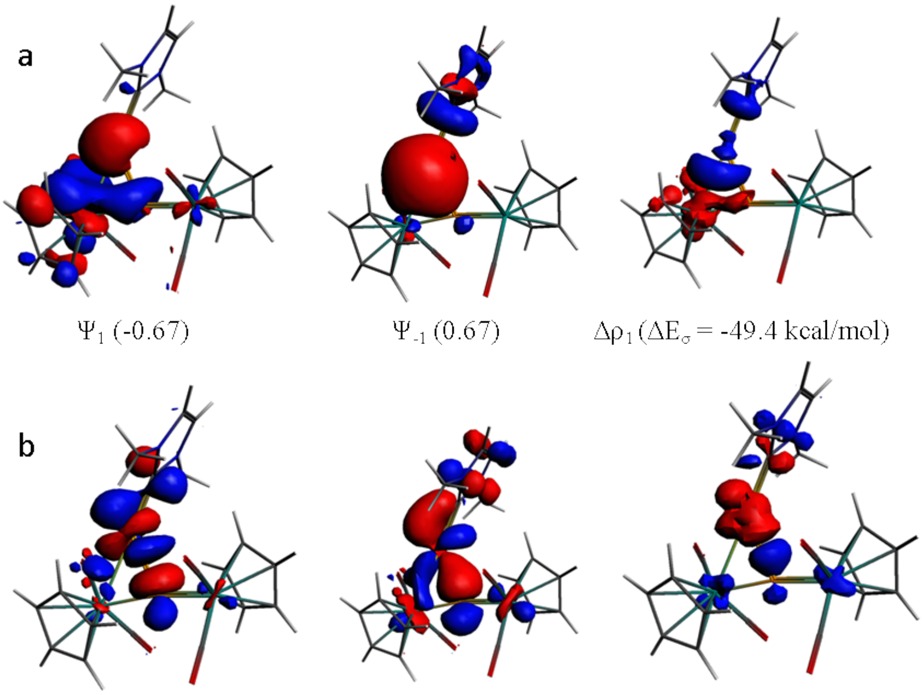

Ψ_1 (-0.67) Ψ_{-1} (0.67) $\Delta\rho_1$ (ΔE_σ = -49.4 kcal/mol)

Ψ_2 (-0.34) Ψ_{-2} (0.34) $\Delta\rho_2$ (ΔE_π = -15.1 kcal/mol)

Supplementary Figure S5. Plots of relevant bonding NOCV pairs (Ψ_n/Ψ_{-n}) for **2a$_{\mathbf{IMe}}$** ($Cp_2(CO)_4Mn_2$)B-Au(IMe)) with accompanying eigenvalues, the associated deformation densities ($\Delta\rho_n$) and the orbital stabilization energies (ΔE) corresponding to (a) σ-donation and (b) π-back donation. Positive and negative eigenvalues correspond to bonding and antibonding interactions, respectively. The direction of charge flow in the deformation densities is from red → blue. IMe = N,N'-dimethylimidazol-2-ylidene.

Table S1. Coordinates of the B3LYP/6-311G(d),LANL2DZ optimized geometry of **3**, used in the simulation of FT-IR data

Center	**X**	**Y**	**Z**
Mn	-1.396227	2.060889	0.155470
Hg	1.116207	-0.552576	-0.125753
B	-1.301424	0.243965	-0.033317
O	-3.817310	1.462218	1.689564
C	-2.855430	1.711755	1.096725
Mn	-1.442871	-1.702386	-0.121235
O	0.340778	1.921707	2.515734
C	-0.355305	1.980255	1.590186
C	-2.683946	-1.101304	-1.240322
O	-3.516864	-0.745466	-1.951357
C	-0.577894	-2.386801	-1.547397
O	-0.109537	-2.904504	-2.464938
C	-0.705242	4.052516	-0.502632
H	-0.193388	4.747554	0.146867
C	-0.084867	3.039771	-1.295633
H	0.978023	2.866833	-1.382049
C	-1.112703	2.335755	-1.984363
H	-0.970709	1.537350	-2.698033
C	-2.361824	2.898328	-1.603654
H	-3.332714	2.579383	-1.952514
C	-2.102513	3.968617	-0.693986
H	-2.847717	4.585734	-0.213938
C	-1.622897	-1.653484	2.049731
H	-1.436355	-0.789922	2.670288
C	-0.674319	-2.663422	1.709770
H	0.348190	-2.719148	2.054055
C	-1.342539	-3.637183	0.914832
H	-0.892569	-4.524053	0.492566
C	-2.692158	-3.234440	0.757969
H	-3.454500	-3.766092	0.208200
C	-2.868566	-2.007883	1.468463
H	-3.782038	-1.437401	1.547584
C	3.281261	-0.029696	0.023218
C	4.235565	-0.622091	-0.811833
H	3.942075	-1.351332	-1.561698
C	5.586012	-0.286122	-0.699057
H	6.314540	-0.753723	-1.355155
C	5.997693	0.644950	0.251761
H	7.047784	0.905750	0.340205
C	5.056141	1.239389	1.088808
H	5.369739	1.965734	1.833001
C	3.705233	0.904953	0.975673
H	2.990917	1.382206	1.639970

Table S2: Coordinates of the OLYP/TZP,QZ4P optimized geometry of **3**, used in ETS-NOCV analysis and presented in Figure S3.

Center	**X**	**Y**	**Z**
C	3.423130	0.945350	0.940688
C	2.990308	0.068089	-0.062255
C	3.902289	-0.345572	-1.040784
C	5.221185	0.108786	-1.016659
C	5.644901	0.976750	-0.012047
C	4.743715	1.392771	0.966889
H	3.592517	-1.023943	-1.831556
H	5.918769	-0.216263	-1.784539
H	6.672740	1.328771	0.007296

H	5.068144	2.069582	1.753450
H	2.731419	1.287820	1.704754
Hg	0.981618	-0.538200	-0.097178
Mn	-1.391030	-1.732286	-0.048657
C	-2.875239	-2.079160	1.393287
C	-1.719178	-1.551679	2.035097
C	-0.651793	-2.476570	1.833672
C	-1.146172	-3.552063	1.046614
C	-2.521678	-3.314374	0.776984
B	-1.205298	0.188252	-0.019592
Mn	-1.171432	2.005698	0.134239
C	-1.693850	3.876571	-0.779308
C	-0.339513	3.923935	-0.376223
C	0.366479	2.888348	-1.060360
C	-0.564157	2.198870	-1.887607
C	-1.839042	2.806945	-1.714069
C	-2.718116	1.635232	0.856856
O	-3.746030	1.328939	1.338552
C	-0.364489	1.773149	1.671561
O	0.167279	1.554471	2.699660
C	-2.570492	-1.040146	-1.139641
O	-3.376716	-0.608388	-1.870604
C	-0.609520	-2.435533	-1.480674
O	-0.167870	-2.935051	-2.441244
H	0.082470	4.594739	0.356760
H	1.414148	2.655983	-0.947652
H	-0.342852	1.370293	-2.543838
H	-2.759692	2.489636	-2.178891
H	-2.490121	4.505420	-0.410162
H	-1.663840	-0.629395	2.592585
H	0.354256	-2.379680	2.214017
H	-0.566793	-4.389568	0.687247
H	-3.170271	-3.940065	0.182916
H	-3.838883	-1.595740	1.350477

Table S3: Coordinates of the OLYP/TZP,QZ4P optimized geometry of $\mathbf{2a}_{\mathbf{IMe}}$, used in ETS-NOCV analysis presented in Figure S4.

Center	**X**	**Y**	**Z**
Au	-0.947724	-0.535991	-0.245238
C	-2.723399	0.413023	-0.042318
N	-3.451273	0.576832	1.096099
C	-4.466569	1.499089	0.918431
C	-4.378793	1.929792	-0.368843
N	-3.313986	1.254307	-0.938100
H	-5.157098	1.758075	1.704503
H	-4.975191	2.639482	-0.918668
C	-3.170119	-0.107359	2.344753
H	-4.052912	-0.662266	2.667897
H	-2.340401	-0.787091	2.168899
H	-2.874234	0.614081	3.106295
C	-2.843785	1.453548	-2.296680
H	-2.295591	2.393130	-2.369832
H	-2.179662	0.629010	-2.544849
H	-3.695093	1.463030	-2.978148
Mn	1.308287	-1.800286	-0.420251
C	2.844916	-2.466839	0.841202
C	2.443128	-3.534384	-0.015833
C	1.076607	-3.812461	0.255176
C	0.633820	-2.927711	1.276396
C	1.725997	-2.083171	1.633430
C	0.338820	-2.116290	-1.870828

O	-0.193753	-2.386649	-2.882791
C	2.414070	-0.909333	-1.432953
O	3.162468	-0.328084	-2.125796
B	1.124389	0.062635	0.071180
Mn	1.295967	1.816103	0.625303
C	-0.205333	3.033164	-0.282227
C	0.638163	2.468088	-1.280382
C	1.960013	2.941385	-1.053184
C	1.932861	3.796509	0.090170
C	0.602114	3.850868	0.565295
C	2.828896	1.192335	1.168666
O	3.853179	0.730596	1.521510
C	0.523592	1.270651	2.092675
O	0.013282	0.849415	3.071657
H	3.811978	-1.989874	0.859284
H	3.055116	-4.018260	-0.761676
H	0.464272	-4.538098	-0.259403
H	-0.362584	-2.886229	1.688950
H	1.706886	-1.299387	2.374480
H	2.835570	2.657639	-1.615744
H	0.338225	1.795389	-2.068397
H	2.789329	4.273959	0.541941
H	0.261784	4.376953	1.444256
H	-1.256031	2.836523	-0.146965

References

[1] H. Braunschweig, M. Burzler, R. D. Dewhurst and K. Radacki, *Angew. Chem. Int. Ed.* 2008, **47**, 5650.

[2] Compound **3** was found to decompose through time. The small scales on which **3** was synthesized is a result of this instability. Despite the small scales employed, the reaction was found to be reliably reproducible, and was carried out a number of times in order to complete the spectroscopic and analytical procedures reported herein.

[3] G. Sheldrick, *Acta Cryst.* 2008, **A64**, 112.

[4] Gaussian 09, Revision D.01, M. J. Frisch, G. W. Trucks, H. B. Schlegel, G. E. Scuseria, M. A. Robb, J. R. Cheeseman, G. Scalmani, V. Barone, B. Mennucci, G. A. Petersson, H. Nakatsuji, M. Caricato, X. Li, H. P. Hratchian, A. F. Izmaylov, J. Bloino, G. Zheng, J. L. Sonnenberg, M. Hada, M. Ehara, K. Toyota, R. Fukuda, J. Hasegawa, M. Ishida, T. Nakajima, Y. Honda, O. Kitao, H. Nakai, T. Vreven, J. A. Montgomery, Jr., J. E. Peralta, F. Ogliaro, M. Bearpark, J. J. Heyd, E. Brothers, K. N. Kudin, V. N. Staroverov, R. Kobayashi, J. Normand, K. Raghavachari, A. Rendell, J. C. Burant, S. S. Iyengar, J. Tomasi, M. Cossi, N. Rega, J. M. Millam, M. Klene, J. E. Knox, J. B. Cross, V. Bakken, C. Adamo, J. Jaramillo, R. Gomperts, R. E. Stratmann, O. Yazyev, A. J. Austin, R. Cammi, C. Pomelli, J. W. Ochterski, R. L. Martin, K. Morokuma, V. G. Zakrzewski, G. A. Voth, P. Salvador, J. J. Dannenberg, S. Dapprich, A. D. Daniels, Ö. Farkas, J. B. Foresman, J. V. Ortiz, J. Cioslowski, and D. J. Fox, Gaussian, Inc., Wallingford CT, **2009**.